

Research Article

Influence of the Percentage of TiO₂ Doped into SiO₂ Matrix on Photocatalysis

L. M. L. da Silva, F. da C. Silva, A. L. de Carvalho, L. Marçal, M. Saltarelli, E. H. De Faria, L. A. Rocha, P. S. Calefi, K. J. Ciuffi, and E. J. Nassar

Chemistry Department, Universidade de Franca, Avenida Dr. Armando Salles Oliveira, 201—Parque Universitário, 14404-600 Franca, SP, Brazil

Correspondence should be addressed to E. J. Nassar, ejnassar@unifran.br

Received 18 June 2012; Accepted 31 July 2012

Academic Editors: M. C. Garcia-Gutierrez, I. Kholmanov, and J. Majimel

Copyright © 2012 L. M. L. da Silva et al. This is an open access article distributed under the Creative Commons Attribution License, which permits unrestricted use, distribution, and reproduction in any medium, provided the original work is properly cited.

The sol-gel process was employed in the preparation of titania-doped spherical nanosilica for application in photocatalysis. To this end, the silica matrix was doped with 1 and 10% titania, and the catalytic activity of the resulting solids in the degradation of rhodamine was tested. The synthesized materials were thermally treated at 120, 400, and 800°C. Differential thermal analysis did not evidence the titania-phase transition from anatase to rutile. Scanning electron microscopy revealed the formation of monodisperse spherical nanoparticles with sizes varying between 400 and 500 nm. The UV-Vis absorption spectra showed that the silica doped with 10% titania promoted 86% rhodamine degradation within 90 minutes, as compared to 40% in the case of the silica containing 1% titania. The silica matrix was demonstrated to affect the titania-phase transformation.

1. Introduction

Advances in nanotechnology have enabled production of nanosized silica via the sol-gel process, and this material has been widely employed in scientific research as well as in engineering development. Nowadays, the sol-gel technique is the method that is most commonly employed for the synthesis of silica nanoparticles. This route involves simultaneous hydrolysis and condensation of alkoxides, so that silica nanoparticles with several characteristics can be achieved [1]. The advantages of monodispersed nanometric particles have been demonstrated, and their importance for many industrial applications, for example, as catalysts, pigments, or pharmaceuticals, has been shown [2]. The sol-gel methodology is well known for being an easy and quick preparation method, and two routes can be used, namely, the hydrolytic and nonhydrolytic [3]. The hydrolytic sol-gel process is based on the inorganic polymerization of molecular precursors and involves evolution of a polymer through the sol and consequent formation of a network.

The molecular precursor employed in the sol-gel process is essentially an alkoxide, and several combinations can be achieved, depending on the compound that is utilized in the reaction [4, 5]. The nonhydrolytic sol-gel process is based on the condensation reaction between a metallic or semimetallic halide and a metallic or semimetallic alkoxide, thereby generating an oxide [6, 7].

Titanium dioxide exists in two main forms, more specifically anatase and rutile. Countless applications have been described for these different phases, but titanium dioxide is mainly used in catalysis (photocatalysis) [8]. Various literature works have discussed about the photocatalytic efficiency of titania-doped matrices in the case of nanoparticles and thin films [9–11].

Photocatalytic reactions are well established in the literature. In the specific case of titanium oxide, water adsorbed onto the titania surface is homolytically cleaved ($h^+ + H_2O_{\text{adsorbed}} \rightarrow H^+ + \cdot OH$) after the oxide is irradiated with light in the UV wavelength region of 290–380 nm, corresponding to the titania band gap [8]. TiO₂

photocatalysis can be applied to the degradation of a number of organic molecules, including pesticides and dyes, among others [12–15].

In this work the hydrolytic sol-gel route was utilized for preparation of silica doped with 1 and 10% titania, and the obtained material was employed in photocatalysis. The synthesized samples were characterized by thermal analysis, scanning electron microscopy, infrared spectroscopy, and X-ray diffraction. The photocatalytic activity of the prepared materials for the degradation of the dye rhodamine was evaluated by means of UV/Vis absorption spectra.

2. Experimental

2.1. Preparation of the Silica Nanoparticles. Tetraethyl orthosilicate ($\text{Si}(\text{OC}_2\text{H}_5)_4$, TEOS, 98%), titanium isopropoxide ($\text{Ti}(\text{OC}_3\text{H}_7)_4$, isoTi, 99%), and Rhodamine B (95%) were purchased from Sigma-Aldrich. Isopropyl alcohol and ammonium hydroxide were acquired from Merck. Stock solutions of dye were prepared via the dissolution of appropriate amounts of the dye in distilled water.

The silica nanoparticles were obtained by basic catalysis, using 0.11 mol of isopropyl alcohol (solvent), 0.03 mol of ammonium hydroxide in aqueous medium. 3.23 mmol of the alkoxide precursor tetraethyl orthosilicate (TEOS) was added after 3 minutes of magnetic stirring at 40°C. Titanium IV isopropoxide (isoTi) was introduced into the reaction mixture after ten minutes, under continuous magnetic stirring. The samples were centrifuged, washed with ethanol, and dried at 120°C. The silica matrix was then doped with 1 or 10% titania in relation to silica, and the resulting xerogels were calcined at 400 or 800°C.

2.2. Evaluation of the Photocatalytic Activity. The photocatalytic activity of these materials was evaluated through suspension of 50 mg of catalyst in 10 mL of aqueous solution of rhodamine ($10^{-5} \text{ mol}\cdot\text{L}^{-1}$) that was kept under magnetic stirring and artificial UV light (365 nm) at room temperature. The xerogel was separated from the supernatant by centrifugation at 3500 rpm for 15 minutes. The concentration of dye remaining in the supernatant was determined by UV-Vis spectroscopy, using a Hewlett-Packard Model 8453 diode array spectrometer, in absorption maximum at 575 nm, after an time of 15, 45, 60, and 90 minutes.

2.3. Characterization of the Catalysts. Thermal Analyses were carried out using a Thermal Analyst TA Instrument SDT Q600 Simultaneous TGA/DTA/ DSC, in nitrogen, at a heating rate of 20°C/min, from 25 to 1000°C, under a N_2 flow of 100 mL/min.

X-ray diffraction (XRD) patterns of the powdered samples were acquired on a Shimadzu model XRD 6000 diffractometer.

Scanning electron microscopy (SEM) of the materials was performed in a Carl Zeiss Model EVO 50 Cambridge (UK) microscope. The samples were coated with a thin gold layer using a sputtering method.

The infrared absorption spectra (FTIR) were acquired on a Bomem MB 100 spectrophotometer with Fourier transform, using the KBr pellet technique, with a sample/KBr ratio of 1 : 300.

3. Results and Discussion

The thermogravimetric curves (TG) evidenced occurrence of mass losses up to 600°C, corresponding to approximately 13% of the sample mass. The maximum mass loss took place between 40 and 173°C, which can be ascribed to loss of water and solvent employed in the syntheses. The residual mass loss was detected between 200 and 600°C, which can be ascribed to pyrolysis of organic matter remaining from the alkoxide precursors.

Figures 1 and 2 present the XRD patterns of the SiO_2 powders doped with 1 and 10% TiO_2 , respectively, obtained after treatment at 120, 400, or 800°C for 4 hours.

The XRD patterns of all the samples showed the presence of an amorphous phase (Figures 1 and 2). The samples treated at 800°C displayed peaks at $2\theta = 25.09$ and 36.38° and $2\theta = 25.14^\circ$ for matrices containing 1 and 10% TiO_2 , respectively, which can be attributed to the TiO_2 anatase phase and indicates the presence of very tiny TiO_2 particles on the SiO_2 support. The (110) rutile reflection peak at $2\theta = 27.5^\circ$ was not observed at high temperature (800°C), probably because the silica matrix inhibited TiO_2 transition from the anatase to the rutile phase. Similar results have been reported in the literature [16, 17]. Indeed, formation of the Ti–O–Si bond prevents changes to the O–Ti–O bond angle and alterations in the O–O distance, which are essential for phase transition to occur. So the transition temperature might be raised over 800°C [13].

The supplementary information (See Supplementary Material available online at doi:10.5402/2012/304546) show the SEM images and the corresponding size distributions for the samples containing 1% and 10% TiO_2 doped into the SiO_2 and treated at different calcination temperatures, namely, 120, 400, and 800°C. Monodispersed spherical particles (100–600 nm) were observed for all the samples, and the mean sizes are listed in Table 1.

All the samples were spherical. The micrographs of the samples with 1 and 10% TiO_2 doped into SiO_2 evidenced uniformly monodispersed spherical particles with an average size of 475 and 510 nm, respectively (supplementary information). All the samples prepared with 10% TiO_2 had larger particle size as compared to the materials containing 1% TiO_2 , suggesting formation of a Si–O–Ti network. There were no important differences between the samples calcined at 120 and 400°C. However, the samples calcined at 800°C presented smaller particle size; this is due to loss residue of the syntheses. This should result in smaller particles and is corroborated by the X-ray diffraction pattern in Figure 2(c), which displays the crystalline pattern attributed to the TiO_2 anatase phase for the samples calcined at 800°C.

The mechanism of TiO_2 photocatalysis has been well discussed in the literature. Hanaor and Sorrel [8] have recently published a review on the importance of the photocatalytic material TiO_2 and its two main phases anatase and

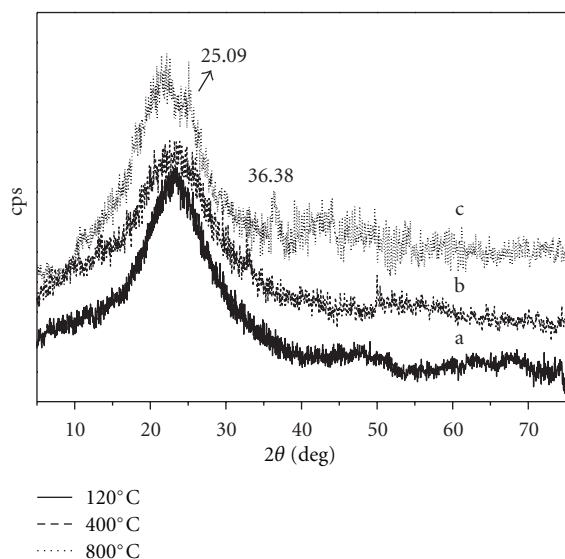


FIGURE 1: X-ray diffraction patterns of the SiO₂ matrix doped with 1% TiO₂ and treated at (a) 120, (b) 400, and (c) 800°C.

TABLE 1: Average particle size for the samples with 1 and 10% TiO₂ doped into SiO₂ matrix and treated at 120, 400, and 800°C.

Heat treatment	% TiO ₂	Mean particle size (nm)
120°C	1	477
	10	513
400°C	1	474
	10	505
800°C	1	415
	10	457

rutile in various photocatalytic processes. Herein, rhodamine photodegradation by the synthesized titania-doped materials was investigated by UV/Vis spectroscopy. The starting rhodamine aqueous solution, 10^{-5} mol·L⁻¹, displayed an absorption band at 553 nm. The effects of the amount of TiO₂ doped into the SiO₂ matrix, calcination temperature, and reaction time on rhodamine photodegradation were then assessed. Figure 3 shows the UV-Vis spectra as a function of irradiation time in the case of the rhodamine sample in the presence of SiO₂ materials doped with 1% TiO₂ and treated at 800°C. Figure 4 summarizes the results of rhodamine degradation in the presence of SiO₂ materials doped with 1% TiO₂ treated at different calcination temperatures, at various reaction times.

UV irradiation at 365 nm was employed during photocatalysis. The absorption maximum did not change during rhodamine degradation in the presence of the SiO₂ materials doped with 1% TiO₂, regardless of the calcination temperature. Degradation was faster during the first 15 min. of reaction, for all the samples. Degradation percentages of 11, 22, and 36% were achieved for the samples treated at 120, 400, and 800°C, respectively. At 90 min., dye degradation was 54% larger for the sample treated at 120°C as compared to the percentage obtained at 15 min. As for the sample calcined

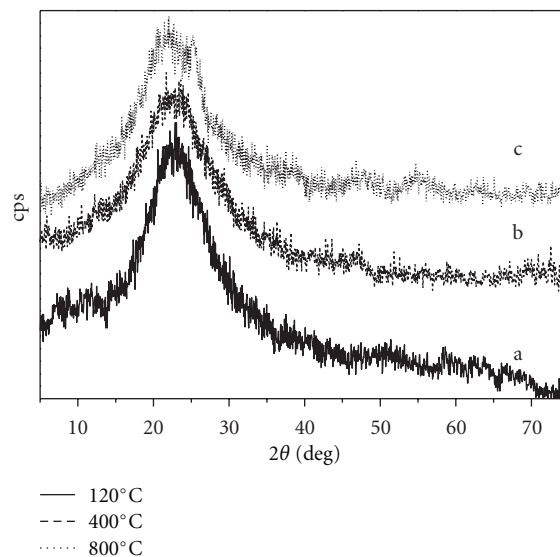


FIGURE 2: X-ray diffraction patterns of the SiO₂ matrix doped with 10% TiO₂ and treated at (a) 120, (b) 400, and (c) 800°C.

at 400°C, degradation at 90 min. was lower as compared to the result achieved at 15 min., but it remained stable. Concerning the sample treated at 800°C, degradation increased by 16% at 90 min. This fact can be ascribed to H₂O and OH groups present on the surface of the TiO₂/SiO₂ matrix. The presence of adsorbed radicals is necessary for photocatalytic reactions. Adsorbed water produces free radicals contain a free unpaired electron and are photogenerated when TiO₂ is exposed to radiation corresponding to its band gap [8]. At the beginning of the reaction, there are many groups able to produce radical species. However, the amount of these species decreases after 15 min., thereby diminishing the percentage of conversion. There is an increase in dye degradation from 15 to 90 min. in the presence of the sample treated at 120°C due to the existence of H₂O and OH groups on the matrix surface.

The anatase phase is described as being a better photocatalyst as compared to the TiO₂ brookite and rutile phases [18]. The anatase phase appears in the sample treated at 800°C, hence accounting for the better rhodamine degradation achieved in this case.

Figure 5 displays the UV-Vis spectra as a function of irradiation time for the rhodamine sample in the presence of SiO₂ materials doped with 10% TiO₂ and treated at 800°C. Figure 6 summarizes the results of rhodamine degradation in the presence of SiO₂ materials doped with 10% TiO₂ treated at different calcination temperatures, at various reaction times.

Rhodamine degradation in the presence of SiO₂ materials doped with 10% TiO₂ is accompanied by a shift in the absorbance band from 553 nm to 549 nm (after 45 min.) and then to 547 nm (after 60 min.). Zhang et al. [19] have ascribed these changes in wavelength to competition between two degradation reactions promoted by the photocatalyst under UV irradiation, namely, rhodamine deethylation and degradation of the rhodamine chromophore structure.

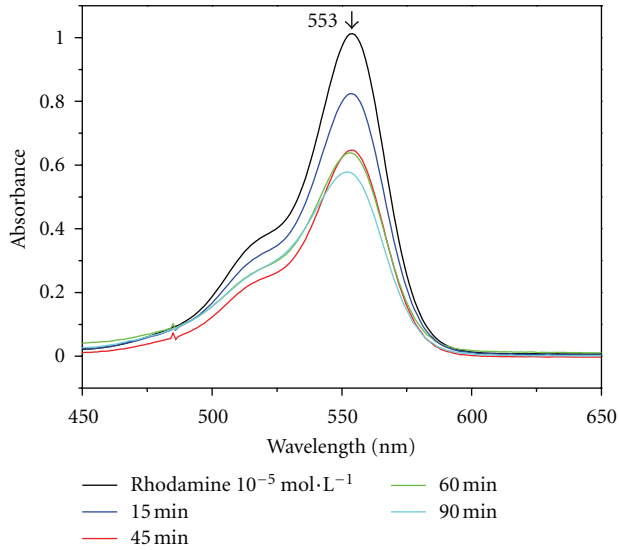


FIGURE 3: Absorption spectra of rhodamine as a function of irradiation time in the presence of SiO_2 materials doped with 1% TiO_2 treated at 800°C .

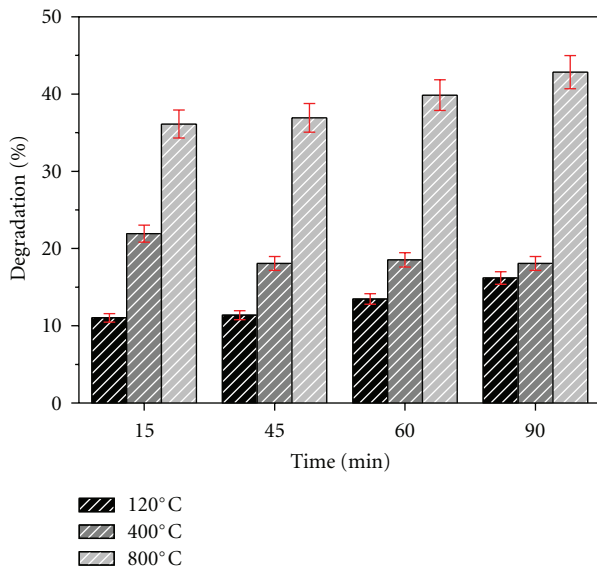


FIGURE 4: Rhodamine degradation results in the presence of SiO_2 materials doped with 1% TiO_2 treated at different calcination temperatures.

According to Watanabe et al. [20], the $\cdot\text{OH}$ radicals preferably react with the aromatic chromophore ring in solution, so rhodamine degradation occurs with no shifts in the absorption band. Deethylation, on the other hand, occurs on the surface of the titania-doped matrix and results in a blue shift of the absorbance band. This indicates that in the case of the samples containing 1% TiO_2 , photocatalysis takes place in solution all the time, whereas for the samples with 10% TiO_2 there is competition between two types of degradation reactions after 15 min.

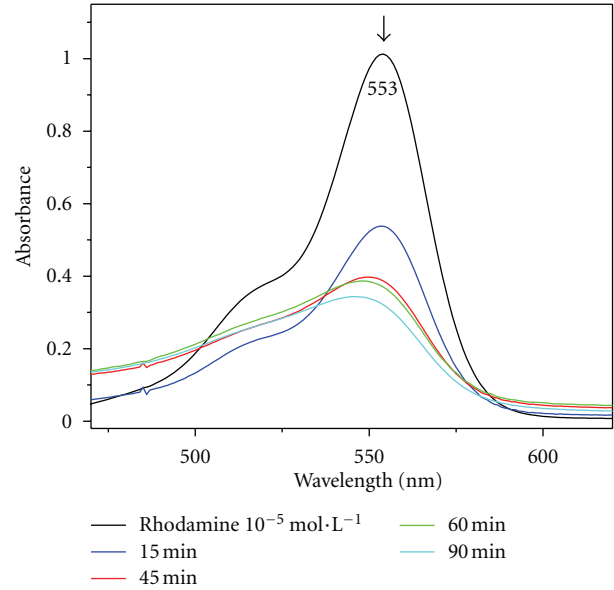


FIGURE 5: Absorption spectra of rhodamine as a function of irradiation time in the presence of SiO_2 materials doped with 10% TiO_2 treated at 800°C .

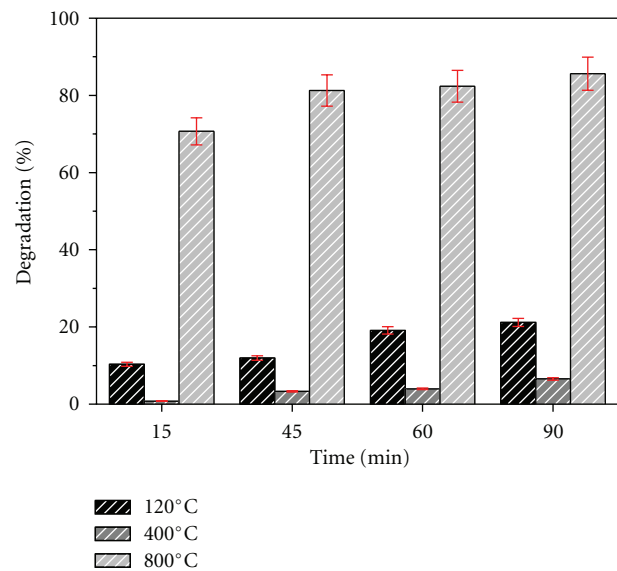


FIGURE 6: Rhodamine degradation results in the presence of SiO_2 materials doped with 10% TiO_2 treated at different calcination temperatures.

The rhodamine degradation reaction in the presence of the material containing 10% TiO_2 was faster within the first 15 min. for the sample treated at 800°C , furnishing 70% dye degradation, which had risen by 21% at 90 min. As for the sample treated at 120°C , the percentage of degradation was the same as that obtained for the sample containing 1% TiO_2 , that is, around 10%, at 15 min. At 90 min., degradation rose by 110%. Photocatalysis in the presence of the sample containing 10% titania and treated at 400°C afforded low

degradation yields: only 6.5% rhodamine was degraded up to 90 min.

The samples with 1 and 10% titania treated at 400°C gave poor results. The former yielded initial degradation of 21%, but this value decreased as a function of time to 18%, and the degradation percentage was very low for the latter sample. As for the samples treated at 120 and 800°C, there was an increase in the degradation percentage as a function of time, but this rise was not directly proportional. It is noteworthy that a tenfold increase in TiO₂ concentration elicited only a twofold rise in degradation.

These results show that the percentage of TiO₂ is not the main factor influencing the rhodamine photodegradation reaction. There are many other parameters, such as TiO₂ particle size and morphology, and the presence of H₂O and OH groups, affecting this reaction.

Prior to the photocatalytic reactions, the infrared spectra of the prepared materials displayed a broad band at 3420 cm⁻¹, ascribed to water molecules and hydroxyl groups, and a band at 1641 cm⁻¹ confirmed the presence of these groups. The shoulder at 1220 cm⁻¹ is attributed to Ti–O–Ti asymmetric stretching [21]. The bands at 1092, 797, and 473 cm⁻¹ correspond to Si–O–Si asymmetric stretching vibration [15, 22–25]. The vibration mode at 954 cm⁻¹ assigned to Si–OH can also be detected before photocatalysis. The latter process is based on the energy of the photons (3.2 eV) from titania to produce very strong oxidizing agents, which in turn are responsible for generation of •OH radicals from water adsorbed onto the surface of the silica or from Si–OH groups. After the photocatalytic reaction, the bands at 3420 and 954 cm⁻¹ decrease, which is evidence that water and/or –OH is necessary for titania photocatalysis to occur, as described by Herrmann [14]. The decrease in the bands due to H₂O and OH groups can explain the degradation percentages obtained in the presence of the materials containing 1 and 10% titania and treated at 800°C. Dye degradation was high at 15 min. of reaction, but increase was not so marked from 15 to 90 min.

4. Conclusion

The results of this work show the importance of temperature, reaction time, percentage of titania in the sample, and presence of water and OH groups for the effectiveness of rhodamine photodegradation. In industrial processes for degradation of polluting dyes, TiO₂ can be diluted into the SiO₂ matrix, thereby reducing costs while promoting good degradation. The samples treated at 800°C gave the best yields, which were achieved during the first 15 minutes of reaction. Thereafter, the percentage of degradation increased no more than 20% of the value obtained at 15 minutes. As for the samples treated at 120°C, degradation percentage increased by approximately 50 and 100% at 90 minutes as compared to 15 minutes for the materials with 1 and 10% TiO₂, respectively. All these observations can be explained by the presence of the H₂O and OH groups on the surface of the SiO₂ nanoparticles doped with TiO₂. In the case of the samples treated at 800°C, the amount of Si–OH

and Ti–OH bonds on the surface of the nanoparticles is lower, as compared to the samples treated at 120°C. Moreover, for materials containing less TiO₂ diluted into SiO₂, pollutant degradation in solution is favored over pollutant deethylation on the matrix surface.

Acknowledgments

The authors acknowledge FAPESP, CNPq, and CAPES (Brazilian research funding agencies) for support of this work and the Microscopy Laboratory of the FFCLRP, São Paulo University, São Paulo, Brazil.

References

- [1] W. Stöber, A. Fink, and E. Bohm, "Controlled growth of monodisperse silica spheres in the micron size range," *Journal of Colloid and Interface Science*, vol. 26, no. 1, pp. 62–69, 1968.
- [2] A. S. de Dios and M. E. Díaz-García, "Multifunctional nanoparticles: analytical prospects," *Analytica Chimica Acta*, vol. 666, no. 1-2, pp. 1–22, 2010.
- [3] J. D. Wright and N. A. J. Sommerdijk, *Sol-Gel Materials Chemistry and Applications*, Taylor & Francis, 2003.
- [4] L. L. Hench and J. K. West, "The sol-gel process," *Chemical Reviews*, vol. 90, no. 1, pp. 33–72, 1990.
- [5] C. J. Brinker and G. W. Scherer, *Sol-Gel Science: The Physics and Chemistry of Sol-Gel Processing*, Academic Press, San Diego, Calif, USA, 1990.
- [6] S. Acosta, R. J. P. Corriu, D. Leclercq, P. Lefèvre, P. H. Mutin, and A. Vioux, "Preparation of alumina gels by a non-hydrolytic sol-gel processing method," *Journal of Non-Crystalline Solids*, vol. 170, no. 3, pp. 234–242, 1994.
- [7] O. J. de Lima, H. C. Sacco, D. C. Oliveira et al., "Porphyrins entrapped in an alumina matrix," *Journal of Materials Chemistry*, vol. 11, no. 10, pp. 2476–2481, 2001.
- [8] D. A. H. Hanaor and C. C. Sorrell, "Review of the anatase to rutile phase transformation," *Journal of Materials Science*, vol. 46, no. 4, pp. 855–874, 2011.
- [9] L. Ge, M. Xu, M. Sun, and H. Fang, "Fabrication and characterization of nano TiO₂ thin films at low temperature," *Materials Research Bulletin*, vol. 41, no. 9, pp. 1596–1603, 2006.
- [10] H. Shin, H. S. Jung, K. S. Hong, and J.-K. Lee, "Crystal phase evolution of TiO₂ nanoparticles with reaction time in acidic solutions studied via freeze-drying method," *Journal of Solid State Chemistry*, vol. 178, no. 1, pp. 15–21, 2005.
- [11] S. Jin and F. Shiraishi, "Photocatalytic activities enhanced for decompositions of organic compounds over metal-photo-depositing titanium dioxide," *Chemical Engineering Journal*, vol. 97, no. 2–3, pp. 203–211, 2004.
- [12] K. Melghit and S. S. Al-Rabaniah, "Photodegradation of Congo red under sunlight catalysed by nanorod rutile TiO₂," *Journal of Photochemistry and Photobiology A*, vol. 184, no. 3, pp. 331–334, 2006.
- [13] Y. Jin, A. Li, S. G. Hazelton et al., "Amorphous silica nanohybrids: synthesis, properties and applications," *Coordination Chemistry Reviews*, vol. 253, no. 23-24, pp. 2998–3014, 2009.
- [14] J.-M. Herrmann, "Photocatalysis fundamentals revisited to avoid several misconceptions," *Applied Catalysis B*, vol. 99, no. 3-4, pp. 461–468, 2010.
- [15] L. Marçal, E. H. de Faria, M. Saltarelli et al., "Amine-functionalized titanosilicates prepared by the sol-gel process as adsorbents of the Azo-Dye orange II," *Industrial and*

- Engineering Chemistry Research*, vol. 50, no. 1, pp. 239–246, 2011.
- [16] Y. Chen, K. Wang, and L. Lou, “Photodegradation of dye pollutants on silica gel supported TiO₂ particles under visible light irradiation,” *Journal of Photochemistry and Photobiology A*, vol. 163, no. 1–2, pp. 281–287, 2004.
- [17] K. Y. Jung, S. B. Park, and S.-K. Ihm, “Local structure and photocatalytic activity of B₂O₃-SiO₂/TiO₂ ternary mixed oxides prepared by sol-gel method,” *Applied Catalysis B*, vol. 51, no. 4, pp. 239–245, 2004.
- [18] K. Y. Jung and S. B. Park, “Enhanced photoactivity of silica-embedded titania particles prepared by sol-gel process for the decomposition of trichloroethylene,” *Applied Catalysis B*, vol. 25, no. 4, pp. 249–256, 2000.
- [19] Y. Zhang, H. Xu, Y. Xu, H. Zhang, and Y. Wang, “The effect of lanthanide on the degradation of RB in nanocrystalline Ln/TiO₂ aqueous solution,” *Journal of Photochemistry and Photobiology A*, vol. 170, no. 3, pp. 279–285, 2005.
- [20] T. Watanabe, T. Takizawa, and K. Honda, “Photocatalysis through excitation of adsorbates. 1. Highly efficient N-deethylation of rhodamine B adsorbed to cadmium sulfide,” *The Journal of Physical Chemistry*, vol. 81, no. 19, pp. 1845–1851, 1977.
- [21] C. Zhu, L. Wang, L. Kong et al., “Photocatalytic degradation of AZO dyes by supported TiO₂ + UV in aqueous solution,” *Chemosphere*, vol. 41, no. 3, pp. 303–309, 2000.
- [22] S. Kein, S. Thorimbert, and W. F. Maier, “Amorphous microporous titania-silica mixed oxides: preparation, characterization, and catalytic redox properties,” *Journal of Catalysis*, vol. 163, no. 2, pp. 476–488, 1996.
- [23] H. Zhang and J. F. Banfield, “Thermodynamic analysis of phase stability of nanocrystalline titania,” *Journal of Materials Chemistry*, vol. 8, no. 9, pp. 2073–2076, 1998.
- [24] X. Gao and I. E. Wachs, “Titania-silica as catalysts: molecular structural characteristics and physico-chemical properties,” *Catalysis Today*, vol. 51, no. 2, pp. 233–254, 1999.
- [25] E. J. Nassar, C. R. Neri, P. S. Calefi, and O. A. Serra, “Functionalized silica synthesized by sol-gel process,” *Journal of Non-Crystalline Solids*, vol. 247, no. 1–3, pp. 124–128, 1999.



Hindawi

Submit your manuscripts at
<http://www.hindawi.com>

